Relative intensity noise and emission linewidth of polariton laser diodes

Marlene Glauser and Raphaël Butté*

Institute of Condensed Matter Physics, Ecole Polytechnique Fédérale de Lausanne (EPFL), CH-1015 Lausanne, Switzerland

(Received 27 May 2013; revised manuscript received 22 July 2013; published 13 September 2013)

We study the relative intensity noise (RIN) per unit bandwidth in polariton laser diodes (LDs) for two pumping geometries, namely, the direct electrical and the intracavity ones as originally described in I. Iorsh *et al*. [Phys. Rev. B **86**, 125308 (2012)], by using rate equations including Langevin noise sources that are adapted from equations employed to describe conventional semiconductor LDs. The obtained expressions for the RIN, which can be used for all inorganic semiconductor polariton LDs, are specifically applied to the case of III-nitride devices. It is highlighted that for frequencies larger than the relaxation resonance frequency the expected minimum RIN of polariton LDs—whatever the pumping geometry—is equal to the standard quantum limit ($\frac{2h\nu}{P_0}$). The general RIN line shape as a function of frequency and optical output power is discussed for the two geometries and simplified expressions for the RIN are given. Then a comprehensive account of the expected evolution of the linewidth of III-nitride polariton LDs upon increasing pumping strength is also given by considering the most advanced theories available to date. The modified Schawlow-Townes linewidth is estimated from the effective ground-state polariton lifetime at threshold, leading to a predicted linewidth as narrow as ∼15 MHz at room temperature for the two pumping geometries when using a consistent set of parameters for III-nitride polariton LDs.

DOI: 10.1103/PhysRevB.88.115305 PACS number(s): 71.36.+c, 03.75.Nt, 42.55.Sa, 42.60.Mi

I. INTRODUCTION

Over the past few years, significant research effort has been devoted to the development of low-threshold coherent light-emitting sources that operate in the strong light-matter coupling regime.[1–5] Soon after the report of this coupling regime occurring in suitably designed planar semiconductor microcavities (MCs),[6] where the eigenmodes are coupled exciton-photon modes called cavity polaritons, it was indeed recognized that such a system could allow the formation of a polariton condensate under incoherent pumping that would be characterized by emission properties sharing similarities with those of conventional laser diodes (LDs) while operating well below the Mott density.[1] Though most of the studies have been carried out under optical pumping, the realization of practical devices will likely rely on an electrical pumping scheme. Initial reports on electrically injected polariton devices dealt with *p-i-n* light-emitting diodes (LEDs) operating in the incoherent light emission regime, i.e., in the absence of macroscopic occupancy of the ground state, that are based on the GaAs material system.[7] Lately, polariton lasing occurring under electrical injection has been reported at cryogenic temperatures, but that relies on a complex geometry involving high external magnetic fields,[8–10] which would prevent any practical implementation of such devices. Though the operation of GaAs-based polariton LEDs has been reported up to room temperature (RT),[11] the robustness of quantum well (QW) excitons in this system is not sufficient to allow for the observation of polariton nonlinearities at such elevated temperatures, as shown by Saba and co-workers through experiments carried out under resonant optical excitation.[12] In recent years wide band gap semiconductors such as GaN (Refs. 4 and 13) or ZnO (Ref. 14) and organic molecules[5] have proven to be suitable active regions to investigate polariton nonlinearities up to RT owing to their high exciton binding energy and large oscillator strength. In a recent article focusing on the prospects for the realization of polariton LDs,[15] it was pointed out that GaN-related MCs operating in the strong coupling regime exhibit several advantages to achieve such devices. This is supported by the recent report of blue-violet III-nitride vertical cavity surface emitting laser (VCSEL) diodes, indicating that significant progress has been made in terms of carrier injection in such vertical emitting devices.[16–19] However, in this latter case it is worth pointing out that a large-threshold current density is required to achieve coherent light emission, which could be circumvented by the realization of polariton LDs.

Recently, we modeled the emission characteristics of polariton LDs using a set of semiclassical Boltzmann equations, which can be applied to various types of inorganic semiconductors, for two relevant pumping geometries that are (i) the direct injection of electrons and holes in the strongly coupled multiple quantum well (MQW) active region and (ii) intracavity optical pumping via an embedded light-emitting diode.[20,21] For a consistent set of parameters corresponding to a GaN cavity with embedded InGaN QWs, a minimum-threshold current density $J_{\mathrm{thr,min}}$ of a few A cm^{-2} was derived for the two geometries at RT and at the optimum exciton-photon detuning δ_{opt}, leading to polariton condensation.[22] Subsequently, an approximate quasianalytical model was considered to derive solutions for both the steady-state and high-speed current modulation of these devices.

In this paper, we elaborate on the previous modeling approach to determine the general expression for the relative intensity noise per unit bandwidth (in dB/Hz), $\frac{\mathrm{RIN}}{\Delta f}$, in polariton LDs for the two above-mentioned pumping geometries. Such a parameter is a recognized figure of merit for conventional LDs as it allows to evaluate the impact of instantaneous temporal fluctuations in the photon density, even in the absence of current modulation. Indeed, variations in the output optical power P_0 stemming from fluctuations in the photon density are responsible for a noise floor that can eventually have a detrimental impact for both analog and digital applications, e.g., in terms of bit-error rate in digital applications. To compute $\frac{\mathrm{RIN}}{\Delta f}$ in polariton LDs, we first derive the expression of the spectral density of the output power $S_{\delta P}(\omega)$ using

simplified differential rate equations written in a compact matrix form in a way similar to that developed by Coldren and Corzine, and we evaluate the relevant Langevin noise source spectral densities or correlation strengths.[23] $\frac{\text{RIN}}{\Delta f}$ is then calculated for the two pumping geometries of interest using the same set of parameters that were considered by Iorsh *et al.* at RT and at δ_{opt}.[20] The results are subsequently analyzed and critically compared with those obtained for conventional LDs and VCSELs. Following the treatment of intensity noise, we qualitatively discuss the expected evolution of the emission linewidth of polariton LDs—that results from frequency noise—by considering currently available theories that are extrapolated to the case of III-nitride structures operating at RT.

II. LANGEVIN NOISE SPECTRAL DENSITY FUNCTION AND RELATIVE INTENSITY NOISE

To obtain the expression of $S_{\delta P}(\omega)$, we shall first consider the rate equations describing the exciton reservoir and the ground-state polaritons for the two pumping geometries:[20]

$$\frac{dn_x}{dt} = P_x - \frac{n_x}{\tau_x} - an_x(n_p+1) + ae^{-\beta\Delta_{\text{esc}}}n_pn_x - bn_x^2(n_p+1) - cn'_en_x(n_p+1), \quad (1)$$

$$\frac{dn_p}{dt} = -\frac{n_p}{\tau_p} + an_x(n_p+1) - ae^{-\beta\Delta_{\text{esc}}}n_pn_x + bn_x^2(n_p+1) + cn'_en_x(n_p+1). \quad (2)$$

Those simplified rate equations have been derived after careful comparison with microscopic modeling based on a full set of semiclassical Boltzmann equations for which analytical solutions cannot be obtained. In particular, the a, b, and c scattering rates, defined hereafter, are obviously closely related to the results issued from the above-mentioned microscopic modeling that is known to describe accurately the evolution of the carrier densities in k space.[20,24] Note that the whole analysis can be reduced to a two-level system because the rate equation describing the electron-hole plasma for the direct electrical pumping geometry does not play a relevant role in the following treatment. Here n_x and n_p are the populations of excitons in the reservoir and polaritons in the ground state, respectively. τ_x is the exciton lifetime taken equal to 1 ns, and τ_p is the lifetime of exciton polaritons in the ground state, which is proportional to the cavity photon lifetime τ_{cav} taken equal to 1 ps. a accounts for the acoustic and optical phonon relaxation rates, $\beta = 1/k_BT$, and Δ_{esc} is the characteristic energy splitting between the bottom of the lower polariton branch (LPB) and states beyond the inflection point of the LPB where zero in-plane wave-vector polaritons are scattered, which is a quantity sensitive to the detuning.[22,25] b is the exciton-exciton scattering rate and c is the rate of exciton relaxation mediated by free carriers. Specificities related to each pumping geometry are contained in the parameters P_x and n'_e. Thus for the direct electrical pumping geometry, $P_x = Wn_{e\text{-}h}$, where W is the exciton formation rate from the electron-hole plasma and $n_{e\text{-}h}$ is the electron-hole pair population, which is proportional to the injected current I, and $n'_e = n_{e\text{-}h}$, whereas for the intracavity optical pumping geometry $P_x = \eta_{\text{int}}I/q$, where η_{int} is the internal quantum efficiency of the electrically pumped QWs of the LED region, which is set to 0.9, q is the elementary charge, and $n'_e = Sn_d$, with S the emitting surface area and n_d the density of free carriers per unit surface obtained from the doping level in the strongly coupled region. The normal mode splitting (Ω_{VRS}) of the present structures is taken equal to 45 meV. Justification for the values considered for all the parameters including parameters a, b, and c is readily available in Ref. 20 and those values are also summarized hereafter in Table I.

TABLE I. List of parameters adopted in this paper to compute $\frac{\text{RIN}}{\Delta f}$ in polariton LDs operating at RT (see text and Ref. 20).

	Pumping geometry	
	Intracavity	Electrical
τ_x (ns)	1	
τ_{cav} (ps)	1	
$\tau_{e\text{-}h}$ (ns)	5	
Ω_{VRS} (meV)	45	
δ_{opt} (meV)	−33	−18
$\lvert X_0\rvert^2$	0.20	0.31
Δ_{esc} (meV)	18	12
η_{int}		0.9
η_0	0.6	
$h\nu$ (eV)	2.987	
S (μm^2)	50 × 50	
n_d (cm^{-2})	2×10^{12}	
W (ps^{-1})		0.01
a (ps^{-1})	7×10^{-11}	7.5×10^{-11}
b (ps^{-1})	1×10^{-13}	4×10^{-13}
c (ps^{-1})	2×10^{-17}	2×10^{-17}

Because the subsequent analysis is restricted to polariton devices operating above the lasing threshold, the terms of spontaneous origin can be omitted. In other words, the $(1+n_p)$ terms appearing in the rate equations can be approximated as n_p. To determine $\frac{\text{RIN}}{\Delta f}$, we introduce the Langevin noise sources $F_{n_x}(t)$ and $F_{n_p}(t)$ as the ac driving sources for the exciton reservoir and ground-state polariton populations, respectively. The usual assumption of white noise is made for those sources, which allows to make use of the differential rate equations. The whole treatment is considered for a constant drive current (i.e., $dI = 0$) so that the differential rate equations written in compact matrix form in the frequency domain become

$$\begin{bmatrix} \gamma_{xx}+j\omega & \gamma_{xp} \\ -\gamma_{px} & \gamma_{pp}+j\omega \end{bmatrix} \begin{bmatrix} n_{x1}(\omega) \\ n_{p1}(\omega) \end{bmatrix} = \begin{bmatrix} F_{n_x}(\omega) \\ F_{n_p}(\omega) \end{bmatrix}, \quad (3)$$

where n_{x1}, n_{p1}, F_{n_x}, and F_{n_p} correspond to the components of the noise that fluctuate at frequency ω. Note here that[20]

$$\gamma_{xx} = \frac{1}{\tau_x} + an_{p_\infty} + 2bn_{x_\infty}n_{p_\infty} + cn'_{e_\infty}n_{p_\infty} - an_{p_\infty}e^{-\beta\Delta_{\text{esc}}}, \quad (4)$$

$$\gamma_{pp} = \frac{1}{\tau_p} - an_{x_\infty} - bn_{x_\infty}^2 - cn'_{e_\infty}n_{x_\infty} + an_{x_\infty}e^{-\beta\Delta_{\text{esc}}}, \quad (5)$$

$$\gamma_{xp} = an_{x_\infty} + bn_{x_\infty}^2 + cn'_{e_\infty}n_{x_\infty} - an_{x_\infty}e^{-\beta\Delta_{\text{esc}}}, \quad (6)$$

$$\gamma_{px} = an_{p_\infty} + 2bn_{x_\infty}n_{p_\infty} + cn'_{e_\infty}n_{p_\infty} - an_{p_\infty}e^{-\beta\Delta_{\text{esc}}}, \quad (7)$$

where the ∞ symbol accounts for the steady-state solutions for the exciton reservoir, ground-state polariton, and electron-hole pair populations.

This compact matrix form is identical to that of a conventional semiconductor LD,[23] hence we can readily express $S_{\delta P}(\omega)$ as

$$S_{\delta P}(\omega) = \left(\frac{\eta_0 h\nu}{\tau_p}\right)^2 S_{n_p}(\omega) + 2\mathrm{Re}\left[\left(\frac{\eta_0 h\nu}{\tau_p}\right)\langle n_{p1} F_0\rangle\right] + \langle F_0 F_0\rangle, \quad (8)$$

where η_0 is the optical efficiency of the laser taken equal to 0.6, $S_{n_p}(\omega)$ is the ground-state polariton spectral density, and F_0 is the Langevin noise source for the stream of output photons resulting from the spontaneous decay of ground-state polaritons. This last term is accounting for the fact that the partition noise of photons transmitted outside the cavity differs from that of photons reflected back in. The expression of $S_{n_p}(\omega)$ is given by

$$S_{n_p}(\omega) = \frac{|H(\omega)|^2}{\omega_R^4}\left[\left(\gamma_{xx}^2 + \omega^2\right)\left\langle F_{n_p} F_{n_p}\right\rangle + 2\gamma_{xx}\gamma_{px}\left\langle F_{n_p} F_{n_x}\right\rangle + \gamma_{px}^2\left\langle F_{n_x} F_{n_x}\right\rangle\right], \quad (9)$$

where $H(\omega)$ is the modulation transfer function, which is pumping geometry dependent, and ω_R is the relaxation resonance frequency equal to $\sqrt{\gamma_{px}/\tau_p}$.[20]

In Ref. 20, it was shown that for the electrical pumping geometry $H(\omega)$ has a complicated expression given by

$$H(\omega) = \frac{\gamma_{px}/\tau_p(W + 1/\tau_{e\text{-}h})}{\gamma_{px}[W - cn_{x_\infty}n_{p_\infty}] + \gamma_{xx}cn_{x_\infty}n_{p_\infty}} \times \frac{\gamma_{px}[W - cn_{x_\infty}n_{p_\infty}] + (i\omega + \gamma_{xx})cn_{x_\infty}n_{p_\infty}}{(\gamma_{px}/\tau_p - \omega^2 + i\omega\gamma_{xx})(i\omega + 1/\tau_{e\text{-}h} + W)}, \quad (10)$$

where $\tau_{e\text{-}h}$ is the lifetime of the electron-hole plasma, whereas for the intracavity pumping geometry the expression of $H(\omega)$ is equivalent to that of conventional LDs:

$$H(\omega) = \frac{\gamma_{px}/\tau_p}{(\gamma_{px}/\tau_p - \omega^2 + i\omega\gamma_{xx})}. \quad (11)$$

At this stage, to evaluate $S_{\delta P}(\omega)$ for the two pumping geometries, we need to determine the correlation strengths between the noise sources F_{n_x}, F_{n_p}, and F_0. For this purpose, we still follow the treatment described in Ref. 23, where it is shown that

$$\langle F_i F_i\rangle = \sum R_i^+ + \sum R_i^-, \quad (12)$$

$$\langle F_i F_j\rangle = -\left[\sum R_{ij} + \sum R_{ji}\right], \quad (13)$$

where the R_i^+ and R_i^- terms correspond to the rates of particle flow into and out of the exciton and ground-state polariton reservoirs, respectively, while R_{ij} and R_{ji} describe the rate of particle flows between the two reservoirs. For the sake of illustration, the rates into and out of those reservoirs are displayed in Fig. 1. Using Fig. 1 together with Eqs. (12) and (13), we obtain

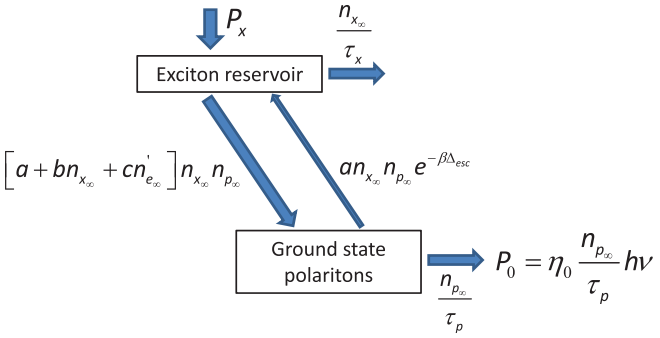

FIG. 1. (Color online) Flowchart reservoir model depicting the flow of particles per unit time based on the rate equations (1) and (2) without the terms of spontaneous origin.

$$\left\langle F_{n_p} F_{n_p}\right\rangle = \frac{2n_{p_\infty}}{\tau_p} + 2an_{x_\infty}n_{p_\infty}e^{-\beta\Delta_{esc}} \approx \frac{2n_{p_\infty}}{\tau_p}, \quad (14)$$

where we used the fact that $\gamma_{pp} = 0$, which is verified when we neglect the terms of spontaneous origin in Eq. (2). This correlation strength is nearly equivalent to that derived for conventional semiconductor LDs, including VCSELs, except for the second term of the middle expression accounting for thermal escape of ground-state polaritons from the condensate, which is inherent to the matterlike character of those bosonic quasiparticles:

$$\left\langle F_{n_x} F_{n_x}\right\rangle = P_x + \frac{n_{x_\infty}}{\tau_x} - \frac{n_{p_\infty}}{\tau_p} + \left\langle F_{n_p} F_{n_p}\right\rangle, \quad (15)$$

$$\left\langle F_{n_p} F_{n_x}\right\rangle = -\left\langle F_{n_p} F_{n_p}\right\rangle + \frac{n_{p_\infty}}{\tau_p}. \quad (16)$$

To determine $S_{\delta P}(\omega)$ we also need to know the dependence of $\langle n_{p1} F_0\rangle$ and $\langle F_0 F_0\rangle$. Transposing the development given in Ref. 23 to the present case, we obtain

$$\langle n_{p1} F_0\rangle = \frac{H(\omega)}{\omega_R^2}[(\gamma_{xx} + j\omega)\langle F_{n_p} F_0\rangle + \gamma_{px}\langle F_{n_x} F_0\rangle], \quad (17)$$

where

$$\left\langle F_{n_p} F_0\right\rangle = -\eta_0\frac{n_{p_\infty}}{\tau_p}h\nu = -P_0 \quad (18)$$

and

$$\left\langle F_{n_x} F_0\right\rangle = 0. \quad (19)$$

This latter correlation strength is equal to 0 because of the absence of correlation between the exciton reservoir noise and the partition noise created by the partially reflecting mirrors.

In addition,

$$\langle F_0 F_0\rangle = h\nu P_0. \quad (20)$$

Using Eqs. (14)–(16) in combination with Eq. (9) and Eqs. (17)–(20), we can now evaluate $S_{\delta P}(\omega)$ given by Eq. (8) for the two pumping geometries. For the intracavity pumping geometry, we obtain

$$S_{\delta P,\mathrm{intra}}(\omega) = h\nu P_0\left[1 + \frac{|H(\omega)|^2}{\omega_R^4}[a_1 + a_2\omega^2]\right], \quad (21)$$

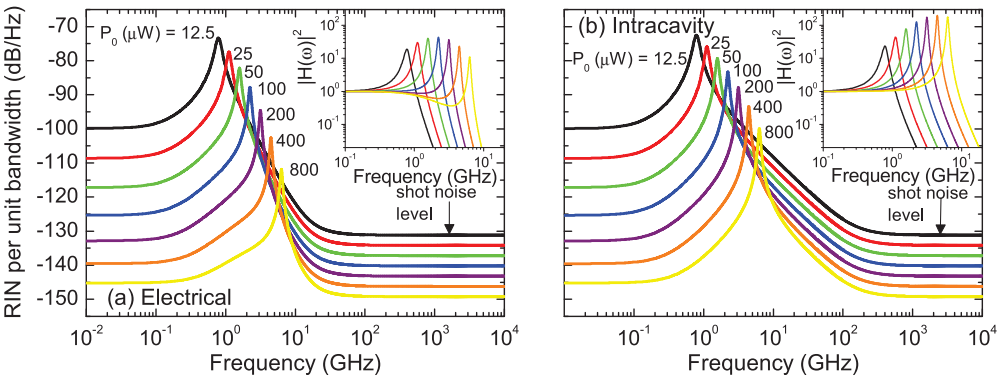

FIG. 2. (Color online) Calculated relative intensity noise as a function of frequency ($\nu = \omega/2\pi$) at different optical output power levels at RT and at δ_{opt} for an InGaN/GaN MQW polariton LD with (a) electrical pumping and (b) intracavity pumping geometries, based on the parameters given in Table I. The insets display the corresponding modulation transfer functions for the same output powers as in the corresponding main figures.

where

$$a_1 = \frac{2\eta_0}{\tau_p}\left[\frac{1}{2n_{p_\infty}}\left(\gamma_{xx}^2\langle F_{n_p}F_{n_p}\rangle + 2\gamma_{xx}\gamma_{px}\langle F_{n_p}F_{n_x}\rangle + \gamma_{px}^2\langle F_{n_x}F_{n_x}\rangle\right) - \gamma_{xx}\omega_R^2\right] \tag{22}$$

and

$$a_2 = \frac{\langle F_{n_p}F_{n_p}\rangle P_0}{h\nu n_{p_\infty}^2} = \frac{2\eta_0}{\tau_p}\left(\frac{1}{\tau_p} + a n_{x_\infty} e^{-\beta\Delta_{\text{esc}}}\right). \tag{23}$$

Once the expression of $S_{\delta P}(\omega)$ is known, we can readily determine $\frac{\text{RIN}}{\Delta f}$ since both quantities are related by

$$\frac{\text{RIN}_{\text{intra}}}{\Delta f} = \frac{2S_{\delta P,\text{intra}}(\omega)}{P_0^2} = \frac{2h\nu}{P_0}\left[1 + \frac{|H(\omega)|^2}{\omega_R^4}[a_1 + a_2\omega^2]\right]. \tag{24}$$

For this pumping geometry, we can point out the close similarity of the RIN expression with that of conventional LDs that only differs via the a_1 and a_2 coefficients.

For the direct electrical pumping geometry, the determination of the expression of the spectral density of the output power $S_{\delta P}(\omega)$ and hence that of $\frac{\text{RIN}}{\Delta f}$ are more tedious because of the form of the modulation transfer function, which is more complex. We finally derive for $\frac{\text{RIN}}{\Delta f}$:

$$\frac{\text{RIN}_{\text{elec}}}{\Delta f} = \frac{2h\nu}{P_0}\left[1 + \frac{|H(\omega)|^2}{\omega_R^4}\left[a_1 + a_2\omega^2 - A' + \frac{2\eta_0}{\tau_p}\gamma_{xx}\omega_R^2\right]\right], \tag{25}$$

where

$$A' = -2\frac{\eta_0}{\tau_p}\omega_R^2\left[C_1\left(C_2^2 + c^2 n_{x_\infty}^2 n_{p_\infty}^2\omega^2\right)\right]^{-1}\left[cn_x n_p\gamma_{xx}\omega^4 + \left(C_2C_3 - C_2\gamma_{xx}^2 + C_2C_4\gamma_{xx} - C_3C_4 cn_{x_\infty}n_{p_\infty} + C_3 cn_{x_\infty}n_{p_\infty}\gamma_{xx} + C_4 cn_{x_\infty}n_{p_\infty}\gamma_{xx}^2\right)\omega^2 + C_2C_3C_4\gamma_{xx}\right] \tag{26}$$

and

$$|H(\omega)|^2 = \frac{C_1^2\left(C_2^2 + c^2 n_{x_\infty}^2 n_{p_\infty}^2\omega^2\right)}{\left(C_3^2 + \gamma_{xx}^2\omega^2\right)\left(C_4^2 + \omega^2\right)}, \tag{27}$$

where the expression of the C_i coefficients with $i \in \{1,4\}$ are given in the Appendix.

The polariton laser RIN is plotted in Figs. 2(a) and 2(b) for the electrical and the intracavity pumping geometries, respectively, based on the parameters listed in Table I and using the expressions given in Ref. 20 for $n_{e\text{-}h_\infty}$, n_{x_∞}, and n_{p_∞}. It can be readily seen that as for conventional semiconductor LDs, the expected minimum RIN of polariton LDs—whatever the pumping geometry—is equal to $\frac{2h\nu}{P_0}$, i.e., to the standard quantum limit, also called shot noise floor. This is the case for the high-frequency range, i.e., for frequencies well above the relaxation resonance frequency. However, contrary to conventional LDs where the excess intensity noise is mostly dominating in the vicinity of ω_R at high output powers, an excess noise is still present at low frequencies ($\omega < 0.1\omega_R$), whose origin will be briefly commented on hereafter. For the electrical pumping geometry it can also be seen that for high optical output power levels, a shoulder (i.e., extra noise) is present on the low-frequency side of the resonance, which is inherited from the nonconventional line shape of the modulation transfer function [cf. the inset of Fig. 2(a)]. In this latter geometry, the peculiar line shape of $H(\omega)$ is also responsible for a sharp decrease in the RIN above ω_R—whose slope increases with output power—leading to a much faster convergence toward the shot noise level than under the intracavity pumping geometry, which exhibits a behavior closer to that of conventional semiconductor LDs with a RIN that falls off at high frequencies at 20 dB/decade before reaching the shot noise level. Note also that the damping of the RIN peak is much more pronounced for polariton LDs having a direct electrical pumping geometry than for the intracavity one. Finally, unlike conventional LDs, the RIN peak gets narrower with increasing optical output power, which is likely due to the absence of an equivalent gain suppression factor in our modeling.[23,26] Indeed, in order to model properly the operating behavior of this former type of devices, the damping factor, which enters in the expression of

the modulation transfer function, includes a phenomenological expression for the gain accounting for saturation phenomena via a gain suppression factor.[23] This decrease in the gain with increasing current induces a broadening of $|H(\omega)|^2$ and hence of the RIN peak, as can be directly inferred from Eq. (24), which is, as we pointed out, fairly similar to that of conventional LDs. The main underlying physical phenomenon responsible for saturation is usually ascribed to intraband carrier relaxation, which leads to a sublinear increase in the intracavity photon density for large currents.[27] In the case of the modeling of polariton LDs, intraband carrier relaxation is at the heart of the semiclassical Boltzmann equations that are computed to derive the evolution of the carrier densities along polariton branches as a function of the pumping rate. Such an effect is thus phenomenologically included in the rate equations (1) and (2), but contrary to the case of conventional LDs it does not induce a broadening of the line shape of the RIN peak with increasing optical output power. However, at this stage we cannot fully discard the contribution of other phenomena that could also induce a behavior similar to that observed for conventional LDs. In particular, it was highlighted by Tassone and Yamamoto that heating of excitons in the reservoir above threshold would decrease the exciton-exciton scattering efficiency, which would subsequently induce an incomplete clamping of n_x.[28] Such an effect could manifest itself in polariton LDs in a way similar to gain suppression in conventional LDs.

In order to get more insights into $\frac{\mathrm{RIN}}{\Delta f}$, we should notice that the expression for the RIN derived for the intracavity pumping geometry can be further simplified when considering the power dependence of the a_1 and a_2 terms [cf. Eq. (24)]. This simplification step is much easier to perform for this latter pumping geometry compared with the electrical one because the modulation transfer function is identical to that of conventional LDs. In this latter case, when only keeping terms in a_1 and a_2 that depend on P_0, we obtain

$$\frac{\mathrm{RIN}_{\mathrm{intra,approx}}}{\Delta f} = \frac{2h\nu}{P_0} + \frac{|H(\omega)|^2}{\omega_R^4}\langle F_{n_p} F_{n_p}\rangle \frac{2}{n_{p_\infty}^2}\left(\frac{1}{\tau_x^2} + \omega^2\right). \tag{28}$$

The suitability of this simplified expression for the RIN in polariton LDs having the intracavity pumping geometry is illustrated in Fig. 3(a), where an excellent agreement is observed between Eqs. (24) and (28) at low output power levels. When setting $\omega = 0$ in Eq. (28), we obtain

$$\frac{\mathrm{RIN}_{\mathrm{intra,approx}}}{\Delta f}(\omega = 0) = \frac{2h\nu}{P_0} + \frac{2h\nu}{P_0}\left[\frac{2}{\omega_R^4}\left(\frac{1}{\tau_p} + a n_{x_\infty} e^{-\beta\Delta_{\mathrm{esc}}}\right)\frac{\eta_0}{\tau_p \tau_x^2}\right], \tag{29}$$

where the second term on the right-hand side decreases as $1/P_0^3$ since $\omega_R^4 \propto P_0^2$. Consequently, this term will rapidly drop below the shot noise floor with increasing power. From Eq. (29), we therefore expect a low-frequency $\frac{\mathrm{RIN}}{\Delta f}$ converging toward the shot noise level. Obviously this is not the case, as can be seen in Figs. 2 and 3(a), because of an irreducible offset introduced by the terms contained in the expression of a_1 [Eq. (22)]. All of them being of similar weight, except for the very last one ($\propto \omega_R^2$) that can be neglected, a tractable analytic expression of the RIN at large optical output powers cannot be readily derived from Eqs. (22)–(24). Finally let us recall that for this specific geometry, the reported high-frequency behavior of the RIN likely should be affected by the cutoff frequency of the pumping LED, which was shown to amount to 3.2 GHz for the set of considered parameters.[20]

As briefly mentioned above, at first sight such a simplified treatment cannot be easily carried out for the electrical pumping geometry due to the complexity of the modulation transfer function. However, when applying Eq. (28) to this geometry with the proper set of parameters, a reasonable agreement is achieved between the exact and the simplified expressions for $\frac{\mathrm{RIN}}{\Delta f}$—especially at low output power—as can be seen in Fig. 3(b), meaning thereby that the qualitative evolution of the latter is, as could be anticipated, governed by the same parameters. Contrary to the intracavity pumping scheme a slight difference can be noticed for the high-frequency tail of the RIN peak, whatever the output power level. In fact, it can be shown that it arises from an extra term that is given in the following improved expression for $\frac{\mathrm{RIN}}{\Delta f}$ under direct electrical pumping that is also displayed in Fig. 3(b):

$$\frac{\mathrm{RIN}_{\mathrm{elec,approx}}}{\Delta f} = \frac{2h\nu}{P_0}\left\{1 + \frac{|H(\omega)|^2}{\omega_R^4}\left[\langle F_{n_p} F_{n_p}\rangle \frac{\eta_0}{\tau_p n_{p_\infty}}\left(\frac{1}{\tau_x^2} + \omega^2\right) - \frac{2\eta_0}{\tau_p}\frac{C_4(\omega_R^2 - \omega^2)\omega^2\omega_R^4}{\omega_R^4 C_4^2 + \omega^2 C_1^2 (c n_{x_\infty} n_{p_\infty})^2}\right]\right\}. \tag{30}$$

III. EMISSION LINEWIDTH

Let us now discuss the expected evolution for the emission linewidth (γ_{polLD}) of a realistic polariton LD such as considered so far, i.e., for a device operating at RT, as a function of the pumping strength P_x. Note that the goal of this section does not consist in providing a detailed account of the calculation of γ_{polLD} that would require a proper quantum optics treatment—which is clearly beyond the scope of the present work—but it rather aims at pointing out the critical parameters that will likely affect γ_{polLD} based on available theories and experiments mostly carried out at low temperature on mature systems.

During the past decade or so, several theoretical approaches have been considered that address the linewidth problem of an optically pumped polariton laser, many of them making an obvious parallel with semiconductor laser theory.[28–34] Those theoretical treatments usually rely on the derivation of the power/emission spectrum that is obtained by taking the Fourier transform of the two-time correlation function of the amplitude of the lower polariton ground state, for which the temporal fluctuations are accounted for by random phase fluctuations in the same way it is done for conventional lasers.[35] Because the above-mentioned analyses are performed by considering a noise-free pump, they can be readily extended to the present electrical injection case. In the limit where the condensate is still weakly populated, those theories converge toward a Schawlow-Townes limited linewidth, i.e., in the noninteracting limit the latter is expected to evolve proportionally to the

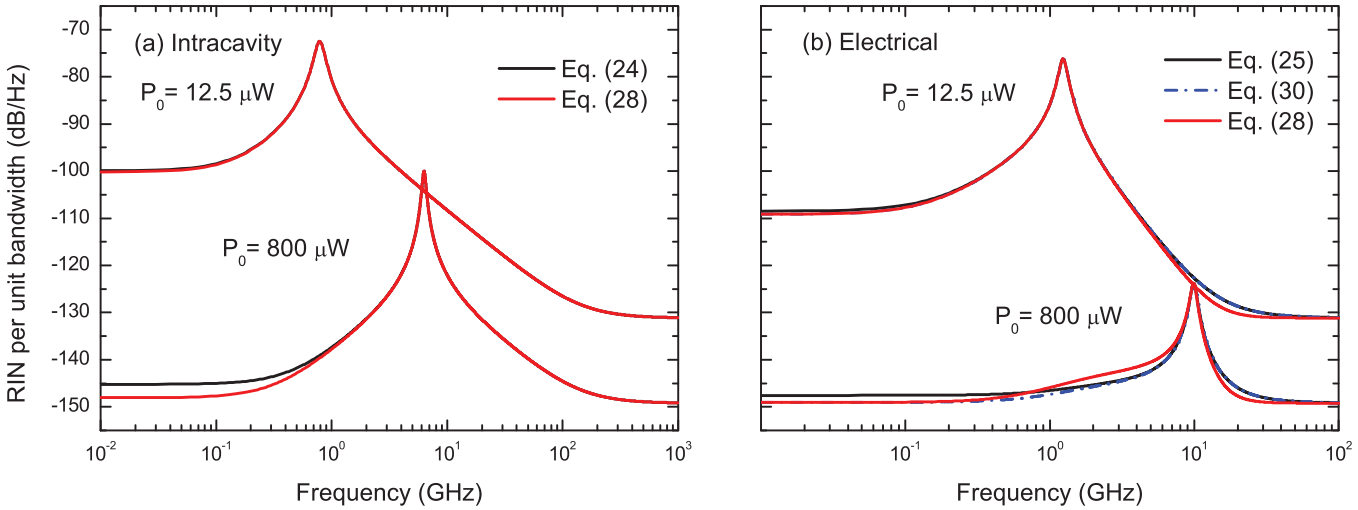

FIG. 3. (Color online) Calculated RIN as a function of frequency ($\nu = \omega/2\pi$) at two different optical output power levels (low and high) at RT and at δ_{opt} for an InGaN/GaN MQW polariton LD for (a) the intracavity pumping geometry using Eqs. (24) (black lines) and (28) (red lines) and (b) for the direct electrical pumping geometry using Eqs. (25) (black lines), (28) (red lines), and (30) (blue dashed-dotted lines). See text for details.

inverse of the number of condensed particles.[28,31,34,36] Note here that number fluctuations are also responsible for an enhancement of the linewidth in the same way it occurs in semiconductor LDs,[37] leading to

$$\gamma_{\mathrm{polLD}} = \gamma_{\mathrm{ST}}(1+\alpha^2), \tag{31}$$

where γ_{ST} is the Schawlow-Townes linewidth and α^2 is the linewidth enhancement factor due to the carrier noise contribution induced by the amplitude to phase coupling terms. However, other parameters have been shown to impact on the $\gamma_{\mathrm{polLD}}(P_x)$ evolution, which are stemming from the interacting nature of polaritons. Thus it was first worked out by Tassone and Yamamoto,[28] and then by Porras and Tejedor,[29] that a self-phase modulation term, which is not present in conventional lasers, should lead to a significant decoherence process in the polariton condensate and hence to a significant increase in the polariton laser linewidth with increasing pumping strength. This increase was shown to remain negligible compared with the Schawlow-Townes linewidth provided $V_{\mathrm{int}} n_{p_\infty} |X_0|^2 \ll \gamma_{\mathrm{ST}}$,[28,29] where $V_{\mathrm{int}} \sim 6E_X^B a_B^2/S$ is the self-interaction occurring in the ground state—which is known to be responsible for the blueshift of the polariton branches—with E_X^B the QW exciton binding energy, a_B the effective Bohr radius, and $|X_0|^2$ is the excitonic fraction of ground-state polaritons.[24,28,38] At this stage, it is worth pointing out that this additional term was first credited to be responsible for the agreement between theory and "early" experiments as the latter displayed a net increase in the linewidth above the condensation threshold of optically pumped MCs that was ascribed to the exciton-exciton mediated interaction occurring in the condensate.[3,4,39–41] However, it turned out that this qualitative agreement was purely fortuitous since initial linewidth measurements led to an overestimate of this parameter due to the significant intensity noise fluctuations of the pump lasers. The true emission linewidth associated with polariton condensates was only made accessible thanks to the use of semiconductor laser diodes free from intensity fluctuations on the ns time scale, leading to a coherence time of 120–150 ps in a CdTe MC at cryogenic temperatures.[36] Reconciliation between theoretical estimates[31,33,34] and experimental results[36] has been obtained via the proper consideration of fluctuations in the number of condensed particles. The impact of the latter is minimized by the replacement of ground-state polaritons escaping from the cavity by high energy lower polaritons. It was shown that the likely related physical mechanism not only originates from stimulated scattering of polaritons from the reservoir but also from nonresonant polariton-polariton scattering processes between the ground state and lower polariton excited states (*a priori* not belonging to the reservoir).[31,33,34,36] The important related aspect is that the time evolution of the ground-state Hamiltonian occurs at a much slower rate than the cavity loss rate, thereby allowing keeping a significant coherence degree that can be directly inferred from the measured decay time $\tau_c^{(2)}$ of the second-order (intensity) correlation function $g^{(2)}(\tau)$.[36] When including such scattering processes, Haug and co-workers[34] showed that the linewidth formula retained a form similar to Eq. (31), where $\alpha^2 = (\frac{\Delta\omega}{\Gamma})^2$, with $\Delta\omega$ is the frequency shift associated with phase fluctuations, and Γ the decay rate of the density fluctuations, which is slowed down due to the above-mentioned nonresonant scattering term. Let us note here that such an evolution of the linewidth does apply to the case of planar microcavities, i.e., in the limit of a large surface emitting area S. However, for sufficiently small mesa structures the energy gap between the polariton ground state and the first excited states can become larger than the energy broadening. In this latter case, the weight of the nonresonant scattering terms is expected to be quenched, thereby leading to a significant linewidth reincrease with increasing pumping strength.[28,34] Note also that for small mesa structures corresponding to small cavity mode volumes, i.e., volumes close to the cube of the emission wavelength, one might potentially expect the Purcell effect to affect in some ways the linewidth of polariton LDs due to the enhancement in the spontaneous emission rate of

excitons. However, as far as III nitrides are concerned, carrier injection in microcavity pillars of reduced diameter, i.e., of dimension close to a micron or even lower, has remained relatively unexplored so far and hence the suitability of such a geometry should be first investigated.

Now that we have recalled the impact of the main terms governing γ_{polLD}, we shall extrapolate their impact on III-nitride polariton LDs operating at room temperature. First, at a given temperature the impact of the self-phase modulation term is expected to be less pronounced in such devices than in their arsenide and telluride counterparts owing to the much smaller size of the Bohr radius in III nitrides, i.e., the magnitude of V_{int} should be smaller than in those two other systems, a comparison already invoked by Kasprzak and co-workers when discussing the differences between CdTe- and GaAs-based MCs.[40] Note also that in III-nitride MCs, recent observations indicate that the LPB blueshift is not only due to the polariton-polariton interaction but also to saturation effects,[25,42] which means that in this system a direct estimate of the injected carrier density will not be straightforward. In addition, it was shown that at RT the δ_{opt} value, corresponding to the minimum pumping strength required for condensation whatever the pumping scheme—namely, an optical[22,25] or electrical[20] one—is negative, meaning thereby that ground-state polaritons are more photonlike than at cryogenic temperatures, where it was shown that $\delta_{\mathrm{opt}} \sim 0$, whatever the material system.[22,25,43,44] As a consequence, the RT excitonic fraction will be smaller than at cryogenic temperatures. Overall this should limit the magnitude of $V_{\mathrm{int}} n_{p_\infty} |X_0|^2$ in III-N polariton LDs. Here we recall that the observed shift of δ_{opt} toward negative δ values with increasing temperature was shown to arise from both a decrease in the relaxation time due to a faster relaxation dynamics,[22,45] and thermal detrapping effects from the bottom of the trap formed in momentum space by the LPB.[22,46] Note that this latter aspect is not included in currently available emission linewidth theories of polariton condensates since they only focus on the low-temperature case. As far as the impact of disorder is concerned, it was highlighted by Whittaker and Eastham[31] that the emission linewidth of polariton condensates might enter into the motional narrowing regime, leading to very long coherence times in MC systems characterized by a low photonic disorder. Though in early III-N MCs grown on a c-plane sapphire substrate the in-plane cavity disorder was known to play a major role,[47] the present III-N polariton LDs would be grown on freestanding GaN substrates,[20] leading to a much better uniformity, as can already be anticipated from the characterization of defect-free nearly lattice-matched InAlN/GaN distributed Bragg reflectors (DBRs)[48] and empty cavities using such DBRs.[49]

In order to be more quantitative and thus provide the readers with some numbers for the III-nitride material system, we can give an expected estimate for γ_{ST}. To this end, we make use of the effective ground-state polariton lifetime at threshold (τ'_p), which can be connected to γ_{ST} in the very same way as it is done for conventional semiconductor LDs.[23] Using the rate equation (2), i.e., that including the terms of spontaneous origin, we can extract the expression of τ'_p, which is given by

$$\frac{1}{\tau'_p} = \frac{1}{\tau_p} - \left[a(1 - e^{-\beta \Delta_{\mathrm{esc}}}) + c n'_{e_\infty} + b n_{x_\infty}\right] n_{x_\infty}, \quad (32)$$

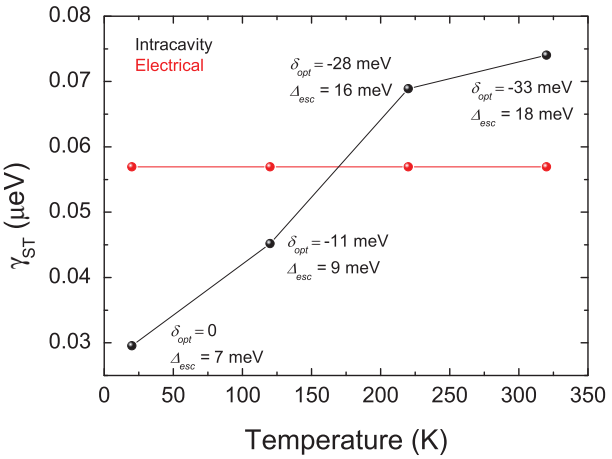

FIG. 4. (Color online) Evolution of the modified Schawlow-Townes linewidth of polariton LDs at optimum detuning as a function of temperature for the electrical (red dots) and the intracavity (black dots) pumping geometry. See text for details.

where the second term on the right-hand side of Eq. (32) is obviously the equivalent for the cavity polariton case to the product of the confinement factor with the group velocity and the material gain per unit length in VCSELs. It describes the increase in the ground-state polariton lifetime resulting from the efficient relaxation of excitons from the reservoir that will compensate for polariton losses. The *modified* Schawlow-Townes linewidth formula when accounting for the 1/2 correction factor[23] is then such that

$$\gamma_{\mathrm{ST}} = \frac{h}{4\pi \tau'_p}. \quad (33)$$

The evolution of γ_{ST} for the two pumping geometries we consider for III-N polariton LDs is displayed in Fig. 4 at the optimum detuning as a function of temperature. Note here that the exact behavior reported for temperatures below 200 K should only be considered as indicative because electrically injected devices become progressively less efficient with decreasing temperature. This is especially true for III-nitride based devices if we take into account the large activation energy (E_A) of Mg, which acts as a deep acceptor ($E_A \in$ 110–190 meV),[50] hence leading to a significant decrease in p-type conductivity when lowering the temperature, which is also due to the concomitant decrease in hole mobility. In particular, the impact of E_A was neglected in the semiclassical Boltzmann treatment, leading to the rate equations (1) and (2).[20] Provided linewidth enhancement effects do not play a significant role, which should be the case at least at cryogenic temperatures according to the most recent theories,[31,34,36] it is predicted that the linewidth of III-N polariton LDs could be as narrow as 5.7×10^{-2} μeV, i.e., 14 MHz at RT. The slightly narrower linewidth predicted for the direct electrical pumping geometry, 5.7×10^{-2} vs 7.3×10^{-2} μeV (18 MHz) for the intracavity one, is likely inherited from the strong dependence of the effective ground-state polariton lifetime given by Eq. (32) on the term proportional to the exciton-exciton scattering rate. The latter is slightly larger for the direct electrical pumping geometry compared with the intracavity one (cf. Table I), which is inherited from the δ_{opt} value that

is closer to zero detuning with this geometry (cf. Table I and Ref. 20). Qualitatively we can understand that when going toward more positive detunings, the critical density leading to condensation increases,[22] hence n_{x_∞}, which subsequently implies an overall decrease in $\frac{1}{\tau_p'}$ ($\frac{1}{\tau_p}$ being already smaller) and thus in γ_{ST}. At such a preliminary stage, we can state that those linewidth values for both pumping geometries should compare favorably with respect to those reported for VCSELs.[51,52]

IV. CONCLUSIONS

In summary, we have carried out an analysis of the relative intensity noise per unit bandwidth in polariton LDs for two relevant pumping geometries, namely, the direct electrical and the intracavity ones, in the framework of a theoretical treatment adapted from that applied to conventional semiconductor LDs using rate equations including Langevin noise sources. The resulting general expressions can be applied to all inorganic semiconductor polariton LDs, but numerical calculations have been performed in the specific case of III-N devices. It was shown that in the high-frequency range the expected minimum RIN of polariton LDs—whatever the pumping geometry—is equal to the standard quantum limit ($\frac{2h\nu}{P_0}$). The general line shape of the RIN as a function of frequency and optical output power has been discussed for the two geometries and approximate (simplified) expressions for the RIN have been given. We have then addressed the expected evolution of the emission linewidth of those devices by considering the most advanced theories available to date. The modified Schawlow-Townes linewidth has been estimated from the effective ground-state polariton lifetime at threshold leading to a predicted linewidth as narrow as ∼15 MHz at RT for the two pumping geometries when using a consistent set of parameters for III-nitride polariton LDs.

ACKNOWLEDGMENTS

We are grateful to Nicolas Grandjean for a critical reading of the manuscript and his continuous support. This work was supported by the NCCR Quantum Photonics, research instrument of the Swiss National Science Foundation, by Grant No. 200020-113542.

APPENDIX

Hereafter we give the explicit expression of the C_i coefficients appearing in Eqs. (26), (27), and (30):

$$C_1 = \frac{\frac{\gamma_{px}}{\tau_p}\left(W + \frac{1}{\tau_{e\text{-}h}}\right)}{\gamma_{px}(W - cn_{x_\infty}n_{p_\infty}) + \gamma_{xx}cn_{x_\infty}n_{p_\infty}}, \tag{A1}$$

$$C_2 = \gamma_{px}(W - cn_{x_\infty}n_{p_\infty}) + \gamma_{xx}cn_{x_\infty}n_{p_\infty}, \tag{A2}$$

$$C_3 = \frac{\gamma_{px}}{\tau_p} - \omega^2 = \omega_R^2 - \omega^2, \tag{A3}$$

and

$$C_4 = W + \frac{1}{\tau_{e\text{-}h}}. \tag{A4}$$

*Corresponding author: raphael.butte@epfl.ch

[1] A. Imamoglu, R. J. Ram, S. Pau, and Y. Yamamoto, Phys. Rev. A **53**, 4250 (1996).
[2] L. S. Dang, D. Heger, R. André, F. Bœuf, and R. Romestain, Phys. Rev. Lett. **81**, 3920 (1998).
[3] J. Kasprzak, M. Richard, S. Kundermann, A. Baas, P. Jeambrun, J. M. J. Keeling, F. M. Marchetti, M. H. Szymańska, R. André, J. L. Staehli, V. Savona, P. B. Littlewood, B. Deveaud, and Le Si Dang, Nature (London) **443**, 409 (2006).
[4] S. Christopoulos, G. Baldassarri Höger von Högersthal, A. J. D. Grundy, P. G. Lagoudakis, A. V. Kavokin, J. J. Baumberg, G. Christmann, R. Butté, E. Feltin, J.-F. Carlin, and N. Grandjean, Phys. Rev. Lett. **98**, 126405 (2007).
[5] S. Kéna-Cohen and S. R. Forrest, Nat. Photonics **4**, 371 (2010).
[6] C. Weisbuch, M. Nishioka, A. Ishikawa, and Y. Arakawa, Phys. Rev. Lett. **69**, 3314 (1992).
[7] A. A. Khalifa, A. P. D. Love, D. N. Krizhanovskii, M. S. Skolnick, and J. S. Roberts, Appl. Phys. Lett. **92**, 061107 (2008); D. Bajoni, E. Semenova, A. Lemaître, S. Bouchoule, E. Wertz, P. Senellart, and J. Bloch, Phys. Rev. B **77**, 113303 (2008); S. I. Tsintzos, N. T. Pelekanos, G. Konstantinidis, Z. Hatzopoulos, and P. G. Savvidis, Nature (London) **453**, 372 (2008).
[8] P. Bhattacharya, A. Das, S. Bhowmick, M. Jankowski, and C.-S. Lee, Appl. Phys. Lett. **100**, 171106 (2012).
[9] P. Bhattacharya, B. Xiao, A. Das, S. Bhowmick, and J. Heo, Phys. Rev. Lett. **110**, 206403 (2013).
[10] C. Schneider, A. Rahimi-Iman, N. Young Kim, J. Fischer, I. G. Savenko, M. Amthor, M. Lermer, A. Wolf, L. Worschech, V. D. Kulakovskii, I. A. Shelykh, M. Kamp, S. Reitzenstein, A. Forchel, Y. Yamamoto, and S. Höfling, Nature (London) **497**, 348 (2013).
[11] S. I. Tsintzos, P. G. Savvidis, G. Deligeorgis, Z. Hatzopoulos, and N. T. Pelekanos, Appl. Phys. Lett. **94**, 071109 (2009).
[12] M. Saba, C. Ciuti, J. Bloch, V. Thierry-Mieg, R. André, Le Si Dang, S. Kundermann, A. Mura, G. Bongiovanni, J. L. Staehli, and B. Deveaud, Nature (London) **414**, 731 (2001).
[13] G. Christmann, R. Butté, E. Feltin, J.-F. Carlin, and N. Grandjean, Appl. Phys. Lett. **93**, 051102 (2008).
[14] Y.-Y. Lai, Y.-P. Lan, and T.-C. Lu, Appl. Phys. Express **5**, 082801 (2012).
[15] R. Butté and N. Grandjean, Semicond. Sci. Technol. **26**, 014030 (2011).
[16] T.-C. Lu, S.-W. Chen, T.-T. Wu, P.-M. Tu, C.-K. Chen, C.-H. Chen, Z.-Y. Li, H.-C. Kuo, and S.-C. Wang, Appl. Phys. Lett. **97**, 071114 (2010).
[17] D. Kasahara, D. Morita, T. Kosugi, K. Nakagawa, J. Kawamata, Y. Higuchi, H. Matsumura, and T. Mukai, Appl. Phys. Express **4**, 072103 (2011).
[18] C. Holder, J. S. Speck, S. P. DenBaars, S. Nakamura, and D. Feezell, Appl. Phys. Express **5**, 092104 (2012).

[19]G. Cosendey, A. Castiglia, G. Rossbach, J.-F. Carlin, and N. Grandjean, Appl. Phys. Lett. **101**, 151113 (2012).
[20]I. Iorsh, M. Glauser, G. Rossbach, J. Levrat, M. Cobet, R. Butté, N. Grandjean, M. A. Kaliteevski, R. A. Abram, and A. V. Kavokin, Phys. Rev. B **86**, 125308 (2012).
[21]The use of a closely related pumping geometry based on a LED and a QW semiconductor laser was recently reported by X. Liu, G. Zhao, Y. Zhang, and D. G. Deppe, Appl. Phys. Lett. **102**, 081116 (2013).
[22]J. Levrat, R. Butté, E. Feltin, J.-F. Carlin, N. Grandjean, D. Solnyshkov, and G. Malpuech, Phys. Rev. B **81**, 125305 (2010).
[23]L. A. Coldren and S. W. Corzine, *Diode Lasers and Photonic Integrated Circuits* (Wiley, New York, 1995), Chap. 5 and Appendix 13.
[24]F. Tassone and Y. Yamamoto, Phys. Rev. B **59**, 10830 (1999).
[25]R. Butté, J. Levrat, G. Christmann, E. Feltin, J.-F. Carlin, and N. Grandjean, Phys. Rev. B **80**, 233301 (2009).
[26]R. Olshansky, P. Hill, V. Lanzisera, and W. Powazinik, IEEE J. Quantum Electron. **23**, 1410 (1987).
[27]E. Rosencher and B. Vinter, *Optoelectronics* (Cambridge University Press, Cambridge, UK, 2002).
[28]F. Tassone and Y. Yamamoto, Phys. Rev. A **62**, 063809 (2000).
[29]D. Porras and C. Tejedor, Phys. Rev. B **67**, 161310(R) (2003).
[30]P. Schwendimann and A. Quattropani, Phys. Rev. B **74**, 045324 (2006).
[31]D. M. Whittaker and P. R. Eastham, Euro. Phys. Lett. **87**, 27002 (2009).
[32]H. Haug, H. T. Cao, and D. B. Tran Thoai, Phys. Rev. B **81**, 245309 (2010).
[33]P. Schwendimann, A. Quattropani, and D. Sarchi, Phys. Rev. B **82**, 205329 (2010).
[34]H. Haug, T. D. Doan, H. T. Cao, and D. B. Tran Thoai, Phys. Rev. B **85**, 205310 (2012).
[35]See, e.g., M. O. Scully and M. H. Zubairy, *Quantum Optics* (Cambridge University Press, Cambridge, UK, 1997). The validity of such an approach relies on the possibility to substitute the electromagnetic field amplitude at the detector position with the polariton ground-state amplitude.
[36]A. P. D. Love, D. N. Krizhanovskii, D. M. Whittaker, R. Bouchekioua, D. Sanvitto, S. A. Rizeiqi, R. Bradley, M. S. Skolnick, P. R. Eastham, R. André, and L. S. Dang, Phys. Rev. Lett. **101**, 067404 (2008).
[37]See, e.g., C. H. Henry, IEEE J. Quantum Electron. **18**, 259 (1982).
[38]C. Ciuti, P. Schwendimann, B. Deveaud, and A. Quattropani, Phys. Rev. B **62**, R4825 (2000).
[39]R. Balili, V. Hartwell, D. Snoke, L. Pfeiffer, and K. West, Science **316**, 1007 (2007).
[40]J. Kasprzak, M. Richard, A. Baas, B. Deveaud, R. André, J.-Ph. Poizat, and Le Si Dang, Phys. Rev. Lett. **100**, 067402 (2008).
[41]J. Levrat, R. Butté, T. Christian, M. Glauser, E. Feltin, J.-F. Carlin, N. Grandjean, D. Read, A. V. Kavokin, and Y. G. Rubo, Phys. Rev. Lett. **104**, 166402 (2010).
[42]G. Rossbach *et al*. (unpublished).
[43]J. Kasprzak, D. D. Solnyshkov, R. André, Le Si Dang, and G. Malpuech, Phys. Rev. Lett. **101**, 146404 (2008).
[44]E. Wertz, L. Ferrier, D. D. Solnyshkov, P. Senellart, D. Bajoni, A. Miard, A. Lemaître, G. Malpuech, and J. Bloch, Appl. Phys. Lett. **95**, 051108 (2009).
[45]J. Levrat, G. Rossbach, R. Butté, and N. Grandjean, in *Physics of Quantum Fluids: New Trends and Hot Topics in Atomic and Polariton Condensates*, edited by A. Bramati and M. Modugno (Springer, Berlin, 2013).
[46]J. Levrat, R. Butté, G. Christmann, E. Feltin, J.-F. Carlin, and N. Grandjean, Phys. Status Solidi C **6**, 2820 (2009).
[47]G. Christmann, D. Simeonov, R. Butté, E. Feltin, J.-F. Carlin, M. Mosca, and N. Grandjean, Appl. Phys. Lett. **89**, 261101 (2006).
[48]G. Cosendey, J.-F. Carlin, N. A. K. Kaufmann, R. Butté, and N. Grandjean, Appl. Phys. Lett. **98**, 181111 (2011).
[49]R. Butté, G. Cosendey, L. Lugani, M. Glauser, A. Castiglia, G. Perillat-Merceroz, J.-F. Carlin, and N. Grandjean, in *III-Nitride Semiconductors and Their Modern Devices*, edited by B. Gil (Oxford University Press, Oxford, UK, 2013).
[50]P. Kozodoy, H. Xing, S. P. DenBaars, U. K. Mishra, A. Saxler, R. Perrin, S. Elhamri, and W. C. Mitchel, J. Appl. Phys. **87**, 1832 (2000).
[51]D. Kuksenkov, S. Feld, C. Wilmsen, H. Temkin, S. Swirhun, and R. Leibenguth, Appl. Phys. Lett. **66**, 277 (1995).
[52]D. Kuksenkov and H. Temkin, in *Vertical-Cavity Surface-Emitting Lasers*, edited by C. Wilmsen, H. Temkin, and L. A. Coldren (Cambridge University Press, Cambridge, UK, 1999), Chap. 6.